PERGAMON

International Journal of Heat and Mass Transfer 46 (2003) 263–272

International Journal of HEAT and MASS TRANSFER

www.elsevier.com/locate/ijhmt

Impingement heat transfer in an under-expanded axisymmetric air jet

M. Rahimi, I. Owen *, J. Mistry

Department of Engineering, The University of Liverpool, Liverpool L69 3GH, UK

Received 5 July 2001; received in revised form 10 July 2002

Abstract

This paper is concerned with the heat transfer that occurs when an underexpanded jet impinges onto a heated surface. The heat transfer in the impingement zone is extremely high and when the surface interferes with the expansion of the jet, the radial distribution of the heat transfer coefficient becomes more complex. If the jet impinges upon the surface before the core of the jet has decayed, there is no longer a maximum stagnation heat transfer coefficient on the geometric axis of the jet, instead a stagnation 'ring' is formed with a radius of about one nozzle diameter. Experimental results are presented for nozzle pressure ratios up to 5.08, and nozzle-to-surface spacings of 3, 6 and 10 nozzle diameters. In addition to the measured data, a clear outcome of the work is that the usual method of representing Nusselt number as a function of Reynolds number is inadequate in compressible flows where the dimensional analysis shows that the nozzle Mach number, or pressure ratio, should also be included.

1. Introduction

There have been many studies of the heat transfer to, or from, an air jet that is impinging onto a surface which is perpendicular to the jet axis. The incentive for these studies is often related to heating and cooling, or drying processes, and the majority are confined to subsonic jets [1,2]. Studies of impinging supersonic jets have mainly concentrated on the gas-dynamics of the jet/surface interaction, sometimes in relation to rocket and jet engine exhausts [3–6]. Considering the number of practical applications where supersonic gas jets impinge upon surfaces and heat transfer is involved, surprisingly little published data is available. This paper considers the heat transfer between a jet of air from a 12.7 mm diameter convergent nozzle, with ratios of nozzle supply pressure to ambient up to 5.08, onto a plane heated surface. Detailed heat transfer measurements have been made for nozzle-to-surface spacings of 3, 6 and 10 nozzle diameters, with some further measurements being made for nozzle-to-surface spacings of 20, 30 and 40.

Although it is relatively simple to place a circular convergent nozzle with a high pressure air supply so the jet impinges normally onto a heated surface, the measurement and representation of the heat transfer characteristics is not so simple. As the air pressure is increased the flow passes from sub- to supersonic and in doing so its characteristics change significantly. When an obstruction is placed into the free jet it will interfere with the flow structure, particularly when it is close to the nozzle exit. Some of the earliest measurements of heat transfer to an impinging jet were made by Gardon and Cobonpue [7] who made the important distinction that in the case of jet speeds which are sufficiently high for the local static temperature in the jet to be changing, the heat transfer coefficient should be defined in terms of the temperature difference between the impingement plate temperature, and the adiabatic wall temperature (a concept that will become clearer later in the paper). Thus:

$$h = \frac{q}{T_w - T_{aw}} \tag{1}$$

Jambunathan et al. [1] tabulate a number of heat transfer studies into circular jets, but with an upper limit

* Corresponding author.
E-mail address: i.owen@liverpool.ac.uk (I. Owen).

0017-9310/03/$ - see front matter
PII: S0017-9310(02)00275-2

Nomenclature

D	nozzle diameter	r	radius of jet
h	heat transfer coefficient	r_5	radius of jet where velocity is half of the maximum
Ma	Mach number		
Nu	Nusselt number	Re	Reynolds number
n	index	T_{aw}	adiabatic wall temperature
P_e	pressure in jet at nozzle exit plane	T_w	wall temperature
P_o	pressure upstream of nozzle	w	jet velocity
P_∞	ambient pressure	z	axial distance from nozzle exit plane
q	surface heat flux		

on Reynolds number of 2.64×10^5. Goldstein et al. [8] investigated the local heat transfer and recovery factor using a 25.4 μm thick stainless steel heating foil with a jet Reynolds number up to 1.24×10^4. Den-Ouden and Hoogendoorn [9] employed temperature-sensitive liquid crystals for Reynolds numbers up to 2.64×10^5. Mohanty and Tawfek [10] used a modified Gardon heat flux sensor for Reynolds numbers up to 3.4×10^4, while Lytle and Webb [11] made a particular study of low nozzle-to-plate spacings, using a heated foil technique and Reynolds numbers up to 3×10^4. Lee et al. [12] used a liquid crystal technique with Reynolds numbers up to 1.4×10^4. The data from these studies, and others, will be compared with results from the present study later in the paper. Although studies such as these have been carried out, in the great majority of cases the jets are subsonic and usually can be considered as incompressible.

2. Experimental apparatus and procedure

Fig. 1 shows a schematic diagram of the test equipment with the nozzle pointing vertically downward onto the instrumented plate. The profile of the convergent nozzle is machined into a 60 mm thick steel plate. The

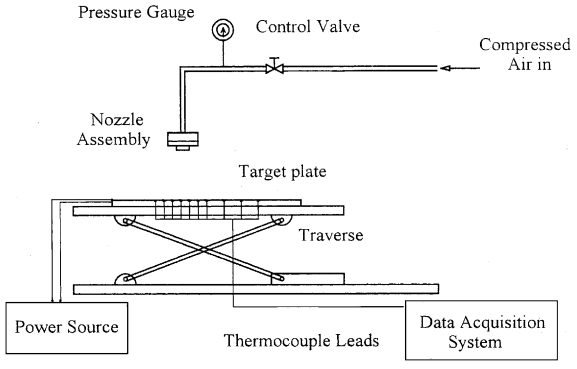

Fig. 1. Schematic diagram of the experimental rig.

temperature and pressure of the air is measured just upstream of the nozzle by a calibrated pressure gauge and a resistance thermometer with uncertainties of ±0.1 bar and ±0.5 °C respectively. The nozzle is held rigidly at the end of a 38 mm diameter supply pipe, while the test plate is held vertically below the nozzle on a table with a three-dimensional traverse. The heated plate was made by carefully gluing a 50.8 μm thick stainless steel foil (36.5 × 190 mm) onto a 10 mm thick wood sheet. K-Type thermocouples were inserted through the back of the wood and were carefully sandwiched between the foil and the wood prior to the foil being glued in place. The technique required some care to ensure good thermal contact between the thermocouple junction and the foil. The exact geometry of the nozzle can have a significant effect on the heat transfer distribution, particularly when the nozzle exit is close to the plate where the velocity profile within the jet will be governed by the nozzle and its upstream conditions. A numerical study of the heat transfer in laminar impinging jets was carried out by Chatterjee and Deviprasath [13] who showed, albeit for very different operating conditions to the present study, that the jet velocity distribution can have a very significant effect on the surface heat transfer. A representation of the nozzle used in the present work is shown in Fig. 2. This nozzle was investigated in great detail by Gibbings [14] who found that the velocity profile at the nozzle exit plane was uniform. A schematic representation of the exit flow obtained by Gibbings et al. [15] using Schlieren photography is shown in Fig. 3.

Fig. 4 shows the position of the foil on the wood, together with the location of the thermocouples. A preliminary test was carried out before the temperature measurements were taken in which the jet was positioned vertically above the middle thermocouple (A) of the closely spaced ones. This was done so that temperatures could be measured along the radius of the impinging jet either side of the jet centre to ensure symmetry. It was important that the jet position was known accurately and, as well as taking care aligning the equipment, a small amount of grease was smeared onto

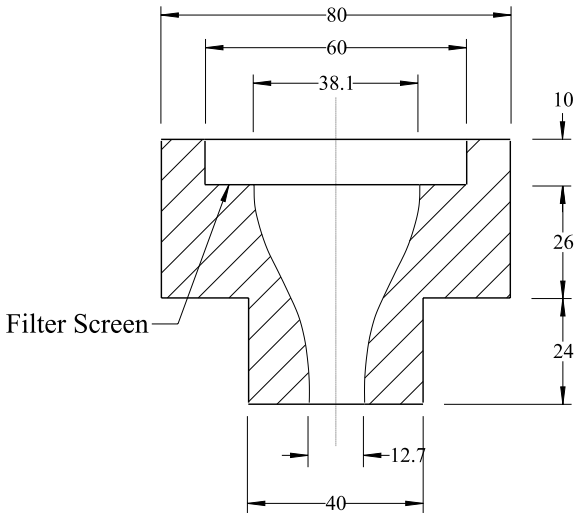

Fig. 2. Nozzle geometry.

the foil and the jet turned on; a mark indicating the centre of the jet could easily be seen. Having confirmed the symmetry of the flow and heat transfer, the jet was positioned above the end thermocouple (B). The closely spaced thermocouples recorded the temperature distribution towards the centre of the jet where the greatest changes were experienced, while the more widely spaced thermocouples were satisfactory for monitoring the temperatures further away from the jet centre. Even so, it was found that the spacing of 6.3 mm between the thermocouples was not close enough but there were practical difficulties of having the thermocouples spaced closer than this. The problem was overcome by taking a set of readings with the jet placed directly above the first thermocouple, and then moving the plate a distance of 3.15 mm in the line of the thermocouples, temperatures were therefore recorded every 3.15 mm. Heating was applied by passing an electric current through the foil. Currents and voltages up to 46 A and 3.66 V respectively were used, the greatest uncertainties in these measurements were ± 1 A and ± 0.1 V respectively. Because of unavoidable conduction heat loss through the wood a detailed analysis of the heat conduction through the wooden substrate was carried out. The greatest effect was found at the greater radii in the heated case (i.e. hottest temperatures) and at the centreline for the unheated case where the coldest temperature was found. At these extreme conditions the greatest effect on the heat flux was found to be less than 5% and this was compensated for in the calculations of heat transfer coefficient. Calculations were also made of the lateral conduction through the foil due to the temperature gradients in the radial direction; this was found to be negligible. A detailed uncertainty analysis showed the uncertainty in the heat transfer coefficient to be about $\pm 6\%$, with a similar uncertainty for the Reynolds numbers.

3. Results and discussion

As discussed earlier, there is not much data available for well-defined conditions, and what there is, is limited by Reynolds number. An experiment was carried out with a Reynolds number of 1.24×10^5 (based on nozzle exit conditions) and a nozzle-to-plate spacing, z/D, of 10. This Reynolds number corresponds to a low (subsonic) pressure ratio $P_o/P_\infty = 1.136$. The experiment was first run with no heating applied to measure the adiabatic wall temperature. Heating was then applied and after the temperatures had stabilised the wall temperatures were again recorded. The results are shown in Fig. 5a where it can be seen that the unheated wall temperature, T_{aw}, is fairly uniform which, as will be seen later, is not the case lin high-speed flows. The resulting Nusselt number

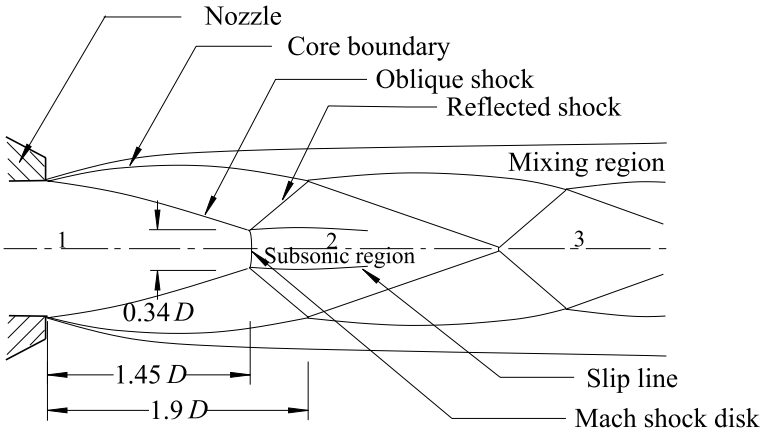

Fig. 3. Jet structure for highly underexpanded jet at $P_o/P_\infty = 5.15$ [14].

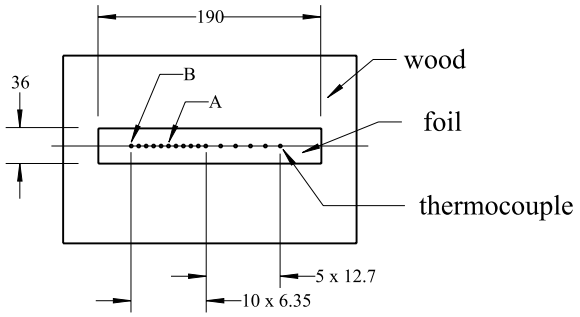

Fig. 4. Arrangement of test plate and thermocouples.

distributions from these measurements are shown in Fig. 5b where they are compared with results of earlier studies that were carried out under similar conditions [8,16,17]. The results, as can be seen, are consistent with each other, thereby giving confidence in the experimental procedure. The Nusselt number was calculated using Eq. (1) and is based on the nozzle diameter and air properties at film temperature $(0.5(T_w + T_{aw}))$.

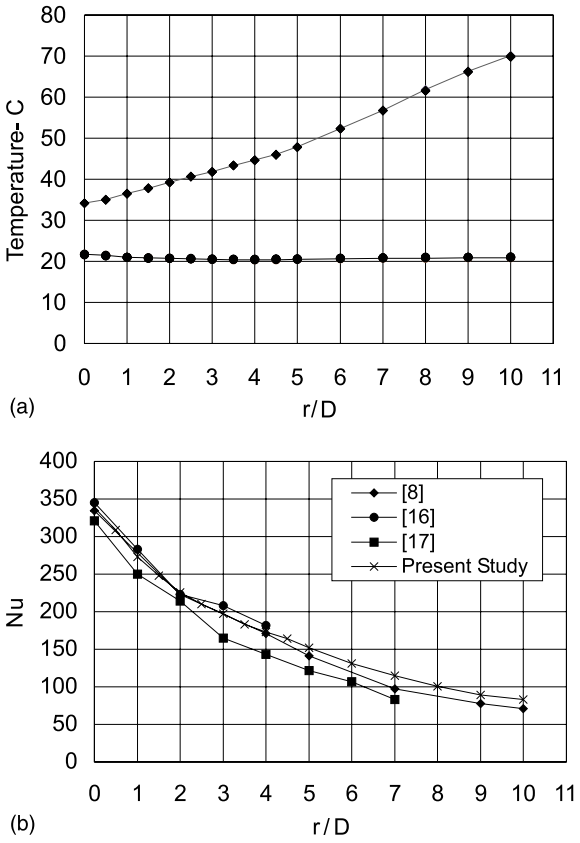

Fig. 5. (a) Heated wall (◆) and adiabatic wall temperature (●) distributions $z/D = 10$, $P_0/P_\infty = 1.136$ and (b) Nusselt number distribution for comparable operating conditions.

This experimental procedure was repeated for increasing air pressures, up to 5.15 bar, $P_o/P_\infty = 5.08$ (although tests were also carried out for pressure ratios up to 6.8, the metal foil suffered damage after a short period and it proved impossible to obtain a full set of data). For the majority of tests the nozzle-to-plate spacings were set at $z/D = 3$, 6 and 10, although some limited data is presented later in Fig. 11 for spacings of 20, 30 and 40. This clearly involved a relatively large number of experiments, and only some of the temperature distributions are shown here as being of interest. Fig. 6 shows the temperature distribution measured on the plate for pressure ratios of 3.04 and 5.08, for $z/D = 3$, 6 and 10. The pressure ratio of 3.08 corresponds to a 'moderately under-expanded jet' as defined by Donaldson and Snedeker [18] while the pressure ratio of 5.08 corresponds to a 'highly under-expanded jet'. The flow structure for a highly under-expanded jet discharging from the nozzle used in the present tests, that was obtained by Gibbings et al. [15], is shown in Fig. 3. The complex cell structure can be seen, together with the position of the Mach disc which, at a pressure ratio of 5.15, was found to be $1.45D$ downstream of the nozzle exit plane.

Considering Fig. 6a, the first feature of note is that the adiabatic wall temperature is no longer constant due to the cooling effect in the high-speed compressible jet. At the lower pressure the stagnation temperature exhibits a local maximum at the centreline. As the jet turns and flows radially along the wall the compressible flow expands and the velocity increases, thereby increasing the cooling effect until the first local minimum at $r/D = 1$. At this position the under-expansion in the jet has been relieved and the radial growth of the wall jet causes the flow to slow thereby leading to an increase in temperature. The temperature then reaches another local maximum before falling to a second local minimum beyond which it increases monotonically to the temperatures at the outer radii (corresponding to ambient temperature in the unheated case). The reason for the second minimum is the subject of some disagreement. Lee and Lee [19] found a similar second peak in the heat transfer distribution for $z/D = 2$, albeit at much lower Reynolds numbers, and attributed it to laminar/turbulent transition. Goldstein et al. [8] noticed a similar effect at $z/D = 2$, again at Reynolds numbers lower than those under consideration here, and attributed it to the formation of vortex rings on the surface due to the fact that the plate is close enough to the nozzle outlet for it to be within the potential core which is surrounded by vortex rings in the shear layer. The formation of this vortex ring around the jet and adjacent to the surface, so the argument goes, leads to a local cooling due to the Ranque-Hilch effect [20]. The present authors are unconvinced by this rather complex argument, not least because the energy separation within a vortex actually leads to the

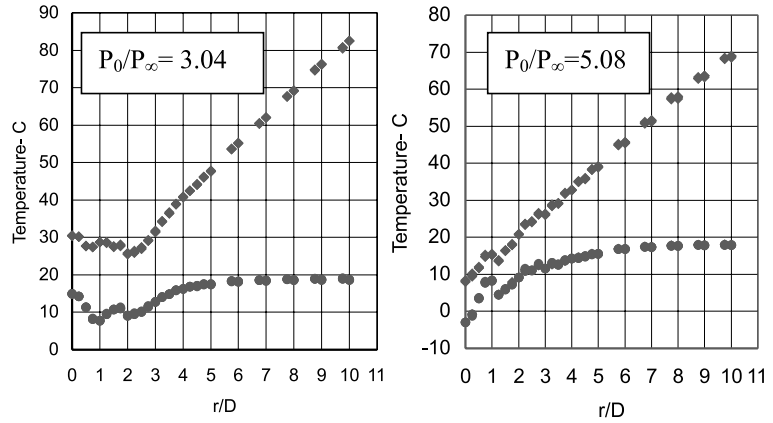

(a) z/D = 3

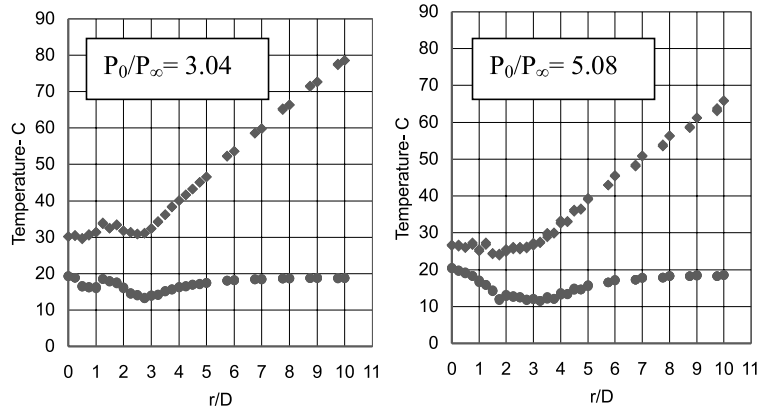

(b) z/D = 6

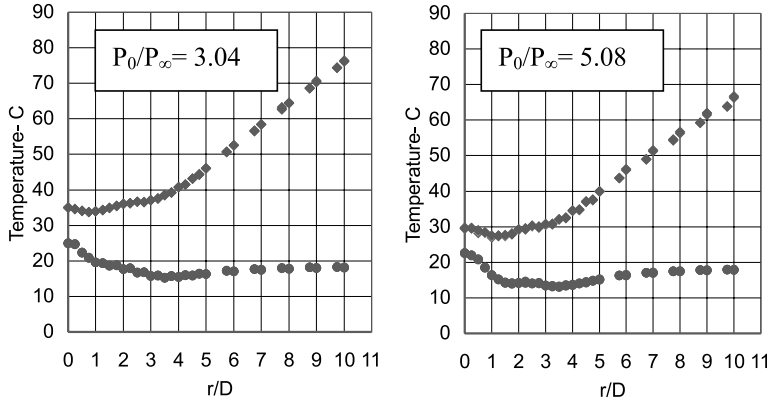

(c) z/D = 10

Fig. 6. Heated (◆) and adiabatic (●) wall temperature distributions.

gas temperature at the outer radius of the vortex being hotter, not cooler. A more convincing argument is found in the results of a numerical study by Behnia et al. [21] who attribute the second peak in the Nusselt number distribution to increased turbulent kinetic energy in this region of the flow. The wall jet has a sharp velocity-peak a short distance from the wall and the lower static temperature in this region of the flow will cause heat transfer from the flow adjacent to the wall, assisted by the increased kinetic energy of turbulence.

Although the hypothesis offered by Behnia et al. is believed to be more convincing, what is clear is that the flow in the case of a compressible jet with small nozzle-to-plate spacings is complex. Further complexity arises when the second case in Fig. 6a is considered. Here the jet is highly under-expanded and the resulting temperature distribution is very different. First, the centreline temperature is a minimum, i.e. no apparent temperature recovery at the stagnation point. Second, there is a local maximum, followed by a second minimum at $r/D \approx 1$. To explain this feature it is necessary to look more closely at the flow field in a highly under-expanded jet (Fig. 3). Fig. 7 has been extracted directly from Donaldson and Snedeker [18] and it shows the normalised velocity profile in a highly under-expanded jet with $P_o/P_\infty = 6.75$. The radius is normalised in the conventional way using the radius r_5 at which the velocity drops to one-half of its maximum value. Far downstream ($z/D > 23.5$) the jet is fully developed with self-similar velocity profiles. However, close to the nozzle outlet, particularly at $z/D = 1.96$ and 3.92, the core of the jet is subsonic, having gone through a disc shock closer to the nozzle, while the surrounding flow is supersonic (refer also to Fig. 3). When a plate is introduced into this flow field the impingement pressure on the axis of the jet will be lower than that in the surrounding annulus. There will, therefore, be a region where the flow is radially inwards towards the central axis as depicted in Fig. 8, again extracted from Donaldson and Snedeker. The same phenomenon was reported by Iwamoto [3] and, by applying a layer of grease to the foil, it was also observed in the present study. The consequence of this flow pattern is that the stagnation point no longer exists at the centre, but as a ring. Returning now to Fig. 6a with the higher pressure

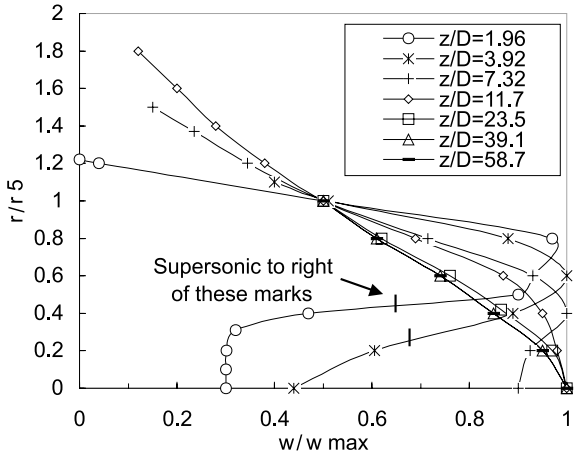

Fig. 7. Normalized velocity distribution for a highly under-expanded jet at different vertical spacing [18].

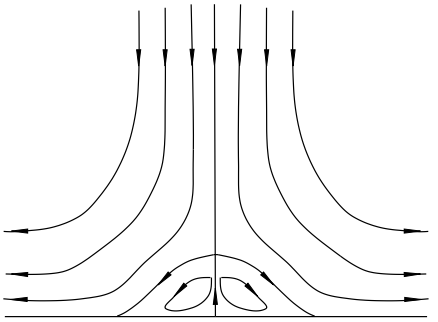

Fig. 8. Flow pattern at separated region of highly under-expanded jet [18].

ratio, the local temperature is at a maximum at $r/D \approx 1$, which will correspond to the shifted stagnation 'point'. The flow will accelerate away from this region, hence leading to a lowering of temperature, and will then slow as the radial jet grows, leading to a corresponding rise in temperature.

At $z/D = 6$, Fig. 6b, the temperature for the lower pressure has a similar form to that shown in Fig. 6a, and a similar explanation will hold. However, for the higher pressure the centreline stagnation point has returned, and there is still evidence of local minima and maxima away from the axis. Whereas the centreline temperature in Fig. 6a was the same as the stagnation temperature upstream of the nozzle, in Fig. 6b it is a few degrees above the nozzle stagnation temperature. This is because the cooler high-speed jet has entrained warmer ambient air into its centre and the stagnation enthalpy is therefore increased. In Fig. 6c the stagnation temperature on the unheated wall is again higher than the ambient temperature and as the radius increases the adiabatic wall temperature falls due to the high-speed of the jet, before increasing to ambient temperature at $r/D \approx 9$, hence the general shape of the adiabatic wall temperature profile seen in Fig. 6c. The temperature distributions for both pressures are similar because the core of the jet has decayed before reaching the surface and the flow complexities are no longer present.

It was found during the course of the experimentation that at certain combinations of supply pressure and nozzle-to-plate spacings, the jet became unstable and the surface temperatures were fluctuating by about 4 °C, whereas in stable conditions the temperatures were steady to within 0.1 °C. This oscillatory instability is known to happen when the presence of the plate interferes with the natural formation of the cell structure within an under-expanded jet [22]. To illustrate the range of the instability Fig. 9 shows the temperature distributions that were taken at different times for apparently the same experimental settings. These settings

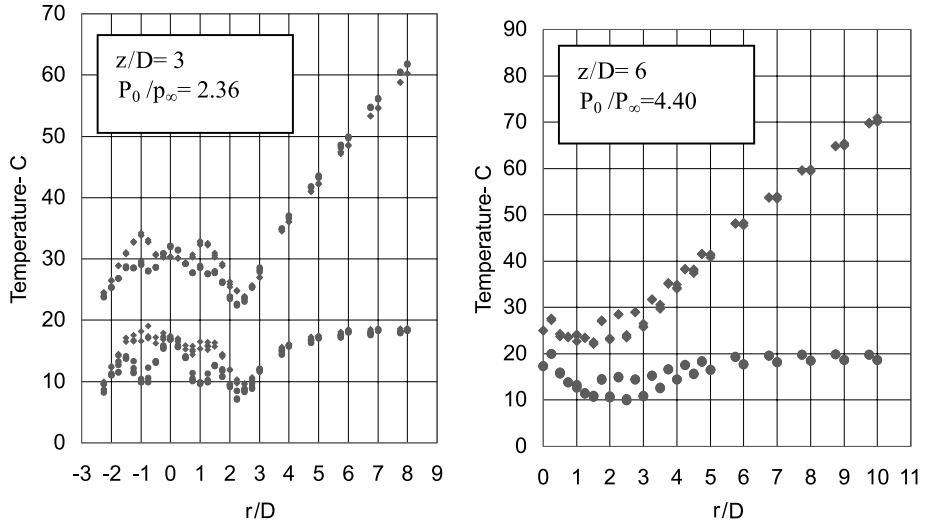

Fig. 9. Variation in heated and adiabatic wall temperature measurements due to flow instabilities.

produced stable temperatures, but were on the border of an unstable condition, and provide yet another example of how the combination of an under-expanded jet impinging onto a plate with short nozzle-to-plate spacing gives rise to complex flow and heat transfer characteristics.

Fig. 10 shows the radial heat transfer distribution for the three nozzle-to-plate spacings and for different nozzle pressures. The shape of these curves, particularly in the impingement zone for the higher pressures at $z/D = 3$, reflects the previous discussion on the temperature profiles. In incompressible flows it is common to assume that the stagnation Nusselt number is proportional to Re^n where n is an experimentally determined constant. In the present work a value of $n = 0.52$ allows the radial distribution of the Nusselt number, away from the impingement zone where compressibility is still influencing the flow, to collapse to a single characteristic. Fig. 10a shows the effects of the subsonic core at the higher pressures, Fig. 10b shows some evidence of the local maxima and minima resulting from the acceleration of the compressible jet, and Fig. 10c exhibits the characteristics similar to a normal impinging subsonic jet, which the jet has become this distance downstream of the nozzle. For $r/D > 2$ all of the profiles show the form expected of subsonic impinging jets, as demonstrated earlier in Fig. 5b. When the nozzle is positioned even further from the surface and the impinging jet is fully developed the radial heat transfer distribution monotonically decreases in the radial direction as shown in Fig. 11.

It is possible to make some comparison between the new data presented here and that in the literature by considering the stagnation point Nusselt number for different Reynolds numbers as shown in Fig. 12. It can be seen that the present study has extended the previously reported data, which is shown for values of z/D varying between 0.5 and 12. To calculate the Reynolds number it is necessary to know the pressure and temperature of the fluid, P_e and T_e, at the plane of the nozzle exit. For pressure ratios, P_o/P_∞ greater than the critical (1.89) the exit conditions have been calculated using isentropic flow equations, and assuming sonic velocity at the nozzle exit plane. i.e.,

$$\frac{P_o}{P_e} = \left\{1 + \frac{k-1}{2}M^2\right\}^{k/(k-1)} \tag{2}$$

and

$$\frac{P_o}{P_e}\left(\frac{T_o}{T_e}\right)^{k/(k-1)} \tag{3}$$

where $M = 1$, $k = 1.4$.

The presentation of the data in the form shown in Fig. 12 highlights a problem with extrapolating from subsonic to supersonic conditions. For supersonic flows the Mach number should appear in the dimensional analysis (as should z/D), giving:

$$Nu = f(Re, Pr, Ma, z/D) \tag{4}$$

When Nu is presented simply as a function of Re, it does not take account of the fact, for example, that a small diameter supersonic jet can have the same Reynolds number as a larger subsonic jet, yet, as we have seen, the heat transfer characteristics can be very different. This means that whoever uses the information such as that presented in this paper, and the others sources that have been referred to, must consider not just similarity based

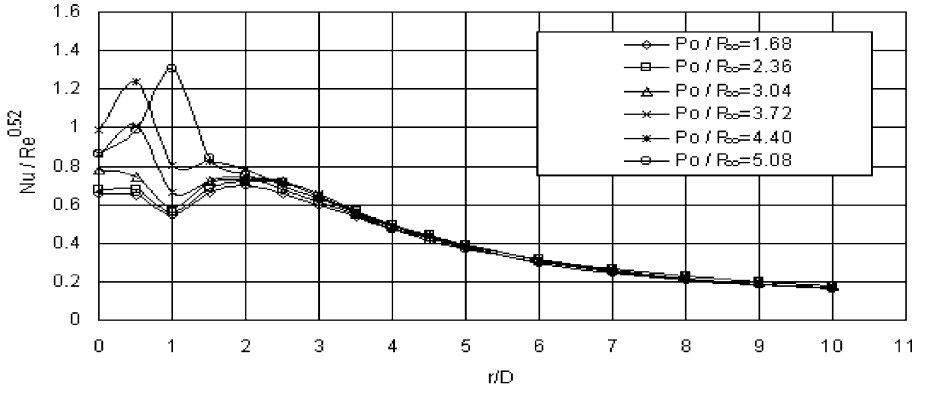

a) z / D = 3

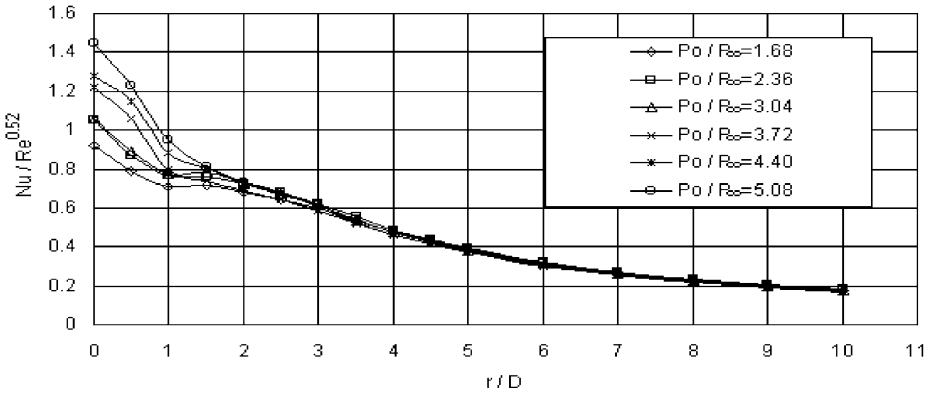

b) z / D = 6

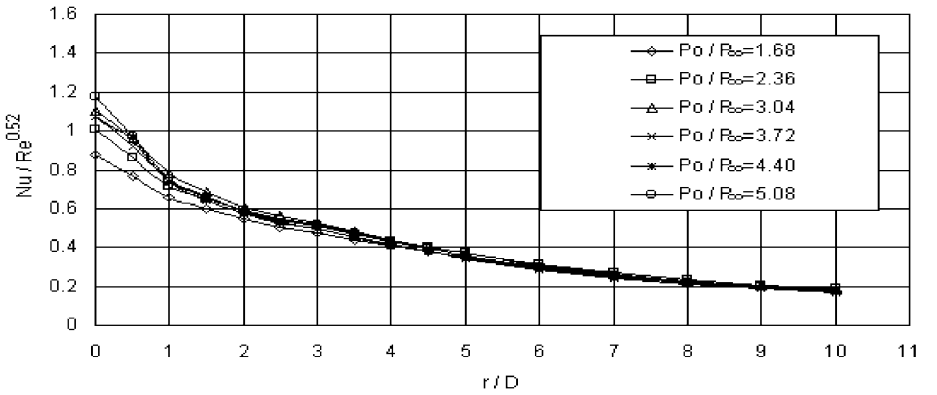

c) z / D = 10

Fig. 10. Radial heat transfer distribution.

on Reynolds and Prandtl number and geometry, but for compressible and supersonic flows they should also seek similarity of pressure ratio. The authors have therefore resisted the temptation to fit a simple *Nu–Re* correlation to the data in Fig. 12 since that would imply that it was appropriate for all sizes of nozzle and Mach numbers, which it clearly is not. The pressure ratios that give rise to the Reynolds numbers for this particular size of jet are also included in Fig. 12. The data for $z/D = 3$ are both the centreline and the maximum Nusselt number.

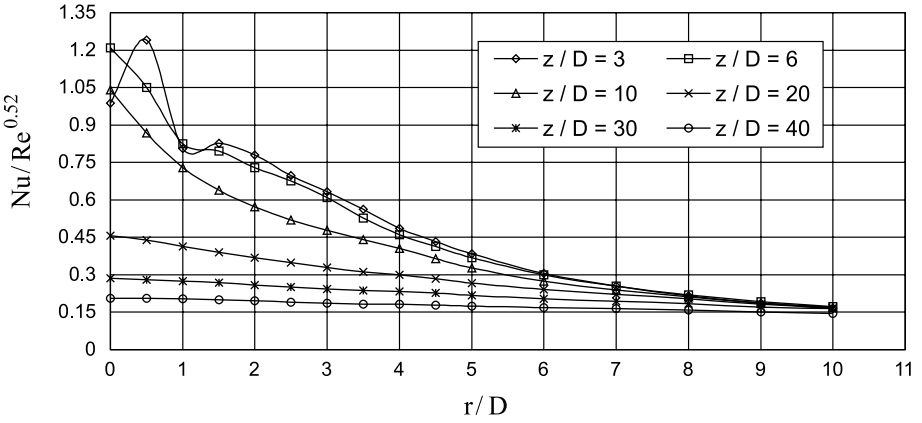

Fig. 11. Heat transfer distribution at different vertical separations $P_0/P_\infty = 4.40$ ($Re = 8.9 \times 10^5$).

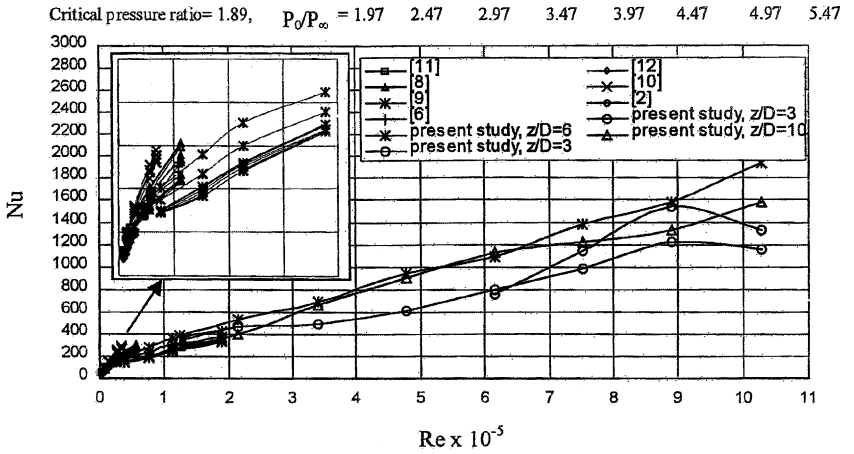

Fig. 12. Stagnation point Nusselt number at different vertical spacing and Reynolds number.

4. Conclusions

This paper has presented experimental data for the heat transfer between an underexpanded jet and a heated surface with uniform heat flux for pressure ratios and Reynolds numbers higher than those previously reported. The stagnation Nusselt number follows the trends of previously published data for lower pressure ratios, but the presenatation of the data in the conventional form of *Nu* vs *Re* is no longer adequate, the nozzle supply to ambient pressure ratio must also be considered. For underexpanded jets there is a core region immediately downstream of the nozzle exit where the flow adjusts to the ambient pressure through a series of normal and oblique shocks, if the impingement surface is within this distance of the nozzle the heat transfer within the impingement zone is complex.

References

[1] K. Jambunathan, E. Lai, M.A. Moss, B.L. Button, A review of heat transfer data for single circular jet impingement, International Journal of Heat and Fluid Flow 13 (2) (1992) 106–115.

[2] J.W. Baughn, S. Shimizu, Heat transfer measurement from a surface with uniform heat flux and impinging jet, Journal of Heat Transfer 111 (1989) 1096–1098.

[3] J. Iwamoto, Impingement of under-expanded jets on a flat plate, Journal of Fluids Engineering 112 (1990) 179–184.

[4] W. Masuda, E. Moriyama, Aerodynamic characteristics of underexpanded coaxial impinging jets, Int J JSME, Series B 37 (4) (1994) 769–775.

[5] P.S. Cumber, M. Fairweather, S.A.E.G. Falle, J.R. Giddings, Predictions of impacting sonic and supersonic jets, Journal of Fluid Engineering 119 (1997) 83–89.

[6] C. Lee, M.K. Chung, K.B. Lim, Y.S. Kang, Measurement of heat transfer from a supersonic impinging jet onto an inclined flat plate at 45 degree, Journal of Heat Transfer 113 (1991) 769–772.
[7] R. Gardon, J. Cobonpue, Heat transfer between a flat plate and jets of air impinging on it, in: International Developments in Heat Transfer, ASME, New York, 1963, pp. 454–460.
[8] R.J. Goldstein, A.I. Behbahani, K.K. Heppelmann, Streamwise distribution of the recovery factor and the local heat transfer coefficient to an impinging circular air jet, International Journal of Heat and Mass Transfer 29 (8) (1986) 1227–1235.
[9] C. Den-Ouden, C.J. Hoogendoorn, Local convective-heat-transfer coefficients for jets impinging on a plate, in: Proceedings of the Fifth International Heat Transfer Conference, JSME, Tokyo, 1974, pp. 293–297.
[10] A.K. Mohanty, A.A. Tawfek, Heat transfer due to a round jet impinging normal to a flat surface, International Journal of Heat and Mass Transfer 36 (6) (1993) 1639–1647.
[11] D. Lytle, B.W. Webb, Air jet impingement heat transfer at low nozzle-plate spacings, International Journal of Heat and Mass Transfer 37 (12) (1994) 1687–1697.
[12] D. Lee, R. Greif, S.J. Lee, J.H. Lee, Heat transfer from a flat plate to a fully developed axisymmetric impinging jet, Journal of Heat Transfer 117 (1995) 772–776.
[13] A. Chatterjee, L.J. Deviprasath, Heat transfer in confined laminar axisymmetric jets at small nozzle-plate distances: the role of upstream vorticity diffusion, Numerical Heat Transfer, Part A 39 (2001) 777–800.
[14] J.C. Gibbings, The combination of a contraction with a supersonic nozzle for a wind tunnel, Ingenieur-Archiv 35 (4) (1966) 269–275.
[15] J.C. Gibbings, J. Ingham, D. Johnson, Flow in a supersonic jet expanding from a convergent nozzle, ARC CP No. 1197, July 1968.
[16] K.K. Kieger, Local and average heat transfer from a flat surface to a single circular jet of air impinging on it, M.Sc. thesis, University of Minnesota, USA, 1981.
[17] E.U. Schlunder, V. Gnielinski, Heat and mass transfer between surface and impinging jet, in: H. Martin (Ed.), Heat and mass transfer between impinging gas jets and solid surfaces, Advances in heat transfer, Vol. 13, 1977, pp. 1–60.
[18] C.D. Donaldson, R.S. Snedeker, A study of free jet impingement part 1. Mean properties of free and impinging jets, Journal of Fluid Mechanics 45 (2) (1970) 281–323.
[19] J. Lee, S.J. Lee, The effect of nozzle configuration on stagnation region heat transfer enhancement of axisymmetric jet impingement, International Journal of Heat and Mass Transfer 43 (2000) 3497–3509.
[20] J.P. Hartnett, E.R.G. Eckert, Experimental study of the velocity and temperature distribution in a high-velocity vortex-type flow, Journal of Heat Transfer (1957) 751–758.
[21] M. Behnia, S. Parneix, P.A. Durbin, Prediction of heat transfer in an axisymmetric turbulent jet impinging on a flat plate, International Journal of Heat and Mass Transfer 41 (12) (1998) 1845–1855.
[22] Y. Sakakibara, J. Iwamoto, Numerical study of oscillation mechanism in under-expanded jet impinging on plate, Journal of Fluid Engineering 120 (1998) 477–481.